OPTIMAL HEATING PROTOCOLS IN FINITE-LENGTH FLAT MICROCHANNELS : THE EFFECT OF RAREFACTION, STREAMWISE CONDUCTION AND VISCOUS DISSIPATION.

Adrover A.
Dipartimento di Ingegneria Chimica, Materiali e Ambiente,
Sapienza, University of Rome,
Rome, 00184,
Italy,
E-mail: alessandra.adrover@uniroma1.it

ABSTRACT

We present an analytical solution of the convection-conduction problem, in laminar flow conditions in finite-length flat microchannels including slip/no-slip flows, effects of rarefaction, streamwise conduction and viscous dissipation, for prescribed wall heat flux boundary conditions.

The solution proposed is valid for low-intermediate Peclet values $Pe \leq 1/\alpha$, α being the microchannel aspect ratio height/length.

The analytical solution is compared with numerical solutions obtained by means of finite-elements method (FEM Comsol 3.5) in a wide range of Pe and α values and for different wall heat flux profiles.

Optimal heating protocols in the presence and in the absence of viscous dissipation are presented.

INTRODUCTION

Focusing on laminar forced convection of an incompressible fluid in a duct, the estimation of transport coefficients requires the solution of the classical Graetz-Nusselt problem. Originally proposed for a sudden step change of the wall temperature at some positions along the duct and no axial diffusion, the Graetz-Nusselt problem is valid for both heat and mass transfer and it has been solved in transient and steady state, for Dirichlet and Neumann boundary conditions, non-Newtonian fluids, high viscous dissipation, boundary condition of continuity between two counterflow streams, axial diffusion, simultaneous heat and mass transfer.

As the size of a channel is reduced, the no-slip boundary condition needs to be modified so that velocity slip and temperature jump may occur at the wall.

The extended Graetz problem in microtubes including effects of rarefaction and viscous dissipation has been recently analyzed by Cetin et al. [1; 2] and by Jeong and Jeong [3; 4] by using eigenfunction expansion (including streamwise conduction) as well as by Tunc and Bayazitoglu [5] using an integral transform technique (neglecting streamwise conduction). The hydrodynamically isothermal developed flow ($T = T_0$ at $z = 0$) is assumed to enter the microchannel of semi-infinite length $z \geq 0$ with uniform wall temperature or uniform heat-flux boundary conditions.

However, this boundary condition at $z = 0$ may be extremely restrictive, especially in the case of laminar velocity profile and low Peclet values [6]. If axial conduction is important, then a sizeable amount of heat is conducted upstream and goes beyond the entrance cross-section $z = 0$ (where non-vanishing boundary conditions apply) into the hydrodynamic development region $z < 0$. Therefore a temperature distribution is built up there which affects the temperature values downstream.

In the present paper we present an analytical solution of the extended Graetz problem in finite-length flat microchannels including effects of rarefaction, streamwise conduction and viscous dissipation. Let $2H$ be channel height (the distance be-

NOMENCLATURE

Br	[-]	Brinkman number
c_p	[J/(KgK)]	Specific heat
F	[-]	Tangential momentum accommodation coefficients
F_T	[-]	Thermal accommodation coefficients
h	[W/(m^2 K)]	Heat transfer coefficient
H	[m]	Half channel height
k	[W/mK]	Thermal conductivity
Kn	[-]	Knudsen number
L	[m]	Length of the channel heated section
L^-, L^+	[m]	Length of upstream and downstream sections
Nu	[-]	Nusselt number
$\langle Nu \rangle$	[-]	Spatial average Nusselt number
Nu_0	[-]	Nusselt number for $Pe/\alpha \to 0$
Nu_∞	[-]	Nusselt number for $Pe/\alpha \to \infty$
Pe	[-]	Cross-sectional Peclet number
$q_w(\zeta)$	[-]	Dimensionless wall heat flux function
T,	[K]	Temperature
T_0	[K]	Inlet temperature at $z = -L^-$
U	[m/s]	Average axial velocity
$v(\eta)$	[-]	Dimensionless axial velocity profile
y,z	[m]	Vertical and axial coordinates

Special characters

α	[-]	Channel aspect ratio
β^-, β^+	[-]	Dimensionless upstream and downstream section lengths
θ	[-]	Dimensionless temperature
θ_b	[-]	Dimensionless bulk temperature
λ	[m]	Molecular mean free path
η, ζ	[-]	Dimensionless vertical and axial coordinates
ρ_f	[Kg/m^3]	Fluid density

tween the two flat plates) and W the channel depth. For a flat microchannel $W >> H$, such that the hydraulic diameter $D_h \to 4H$. The solution, taking into account the presence of the thermal development region, is valid for low-intermediate Peclet values Pe for prescribed heat-flux boundary conditions (no wall conjugation effects).

In the problem formulation, we consider three regions along the microchannel : first a thermally insulated region (length L^-), followed by the heat transfer section with prescribed wall heat flux (length L) and the third one, following the heated section, that is again thermally insulated (length L^+). In this way, since we investigate low-intermediate Peclet values, we can focus on the role of different wall heat flux functions avoiding that the inlet and outlet conditions may influence the Nussel profile in the heated section.

The analytical solution proposed is compared with numerical solutions obtained by means of finite-elements method (FEM Comsol 3.5) in a wide range of Pe and α values and for different wall heat flux profiles. The range of validity of the analytical solution proposed is investigated in detail.

From the temperature field, the local Nusselt axial profile and the average Nusselt number are obtained as a function of the transport parameters i.e. the Peclet number Pe, the Knudsen number Kn, the Brinkman number Br as well as geometrical parameters i.e. the aspect ratio $2H/L$ and the length of upstream section L^-/L.

Performances of different wall-heat flux functions are analyzed in terms of the averaged Nusselt number $< Nu >$. We investigate the best heating protocol in the absence $Br = 0$ and in the presence $Br > 0$ of viscous dissipation.

STATEMENT OF THE PROBLEM

We consider a Newtonian fluid with constant thermodynamic properties entering at $z = -L^-$ a finite-length horizontal microchannel, height $2H$, depth W and total axial length $(L^+ + L + L^-)$, i.e. $-H \le y \le H$, $L^- \le z \le L + L^+$. Let $(2HW)(\rho_f c_p U)T_0$ be the inlet convective flux at $z = L^-$.

The laminar velocity profile, depending exclusively on the cross-section coordinate $\eta = y/H \in [-1,1]$ and satisfying the slip boundary condition $V_z(y) = \mp[(2-F)/F]\lambda(\partial V_z/\partial y)$ at $y = \pm H$ attains the form

$$v(\eta) = \frac{V_z(\eta)}{U} = \frac{3}{2}\frac{(1-\eta^2+4Kn)}{1+6Kn} = \frac{3}{2}(1-\eta^2)\chi + (1-\chi) \quad (1)$$

where U is the average cross-section velocity, $Kn = \lambda/2H$ is the Knudsen number and $\chi = 1/(1+6Kn)$.
We assumed a first order model for rarefaction effects valid for $0.001 \le Kn \le 0.1$ [7] with a tangential moment accommodation coefficient $F = 1$ [5]. The velocity profile reduces to the classical no-slip parabolic velocity profile for $Kn = 0$.

The microtube is thermally insulated for $L^- \le z < 0$ and for $L < z \le L + L^+$. Let $Q_w(z)$ be a prescribed wall heat flux function valid for $0 \le z \le L$. See Figure 1 for a schematic representation of the physical domain and boundary conditions.
Let $Q_{av} = (1/L)\int_0^L Q_w(z)\,dz \neq 0$.

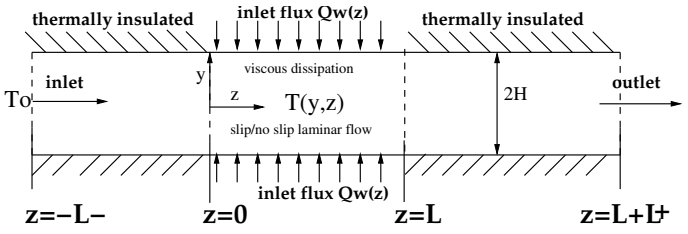

Figure 1. schematic representation of the physical domain and boundary conditions.

By introducing the dimensionless space variables $\eta = y/H$, $\zeta = z/L$ and temperature $\theta = (T - T_0)k/(Q_{av}H)$ the governing steady-state energy equation including the axial conduction and the viscous dissipation terms attains the form

$$-\frac{Pe\,\alpha}{4}v(\eta)\frac{\partial\theta}{\partial\zeta} + \frac{\partial^2\theta}{\partial\eta^2} + \frac{\alpha^2}{4}\frac{\partial^2\theta}{\partial\zeta^2} + 18Br\chi^2\eta^2 = 0\,, -\beta^- \le \zeta \le 1+\beta^+ \quad (2)$$

where the following dimensionless parameters appear

$$Pe = \frac{U\,2H}{k/\rho_f c_p}\,, Br = \frac{\mu U^2}{Q_{av}2H}\,, \alpha = \frac{2H}{L}\,, \beta^- = \frac{L^-}{L}\,, \beta^+ = \frac{L^+}{L} \quad (3)$$

By further introducing the dimensionless axial convective flux $J_c = \frac{Pe\,\alpha}{4}\int_{-1}^{1} v(\eta)\theta(\eta,\zeta)d\eta$ and the dimensionless wall heat flux $q_w(\zeta) = Q_w/Q_{av}$, the following boundary conditions apply

$$J_c|_{\zeta=-\beta^-} = 0\,,\ \left.\frac{\partial J_c}{\partial\zeta}\right|_{\zeta=1+\beta^+} = 12Br\chi^2 \quad (4)$$

$$\left.\frac{\partial\theta}{\partial\eta}\right|_{\eta=0} = 0\,,\ \left.\frac{\partial\theta}{\partial\eta}\right|_{\eta=1} = F_w(\zeta) = \begin{cases} 0 & \text{for } -\beta^- \le \zeta < 0 \\ q_w(\zeta) & \text{for } 0 \le \zeta \le 1 \\ 0 & \text{for } 1 < \zeta \le 1+\beta^+ \end{cases} \quad (5)$$

The outlet boundary condition at $\zeta = 1+\beta^+$ is an integral version of the Danckwertz outlet boundary condition, usually adopted for finite length channels, and implies zero conductive axial heat flux at the outlet section. Its integral version (integral over the channel cross section) allows us to take into account the heat generated by viscous dissipation and is in agreement with the asymptotic condition usually adopted for infinitely long channels.

ANALYTICAL SOLUTION

At low-intermediate values of the Peclet number, the temperature profile exhibits a weak dependence on the vertical coordinate η so that we can reasonably assume that the dimensionless temperature can be written as

$$\theta(\eta,\zeta) = \theta_b(\eta) + \phi(\eta,\zeta)\,, \quad \theta_b(\eta) = \frac{1}{2}\int_{-1}^{1}\theta\,v(\eta)d\eta \quad (6)$$

where $\theta_b(\zeta)$ is the dimensionless bulk temperature and ϕ is an auxiliary function, satisfying the integral constrain $\frac{1}{2}\int_{-1}^{1}\phi(\eta',\zeta)\,v(\eta')d\eta'=0$ and accounting for the temperature dependence on the vertical coordinate i.e. $\partial\theta/\partial\eta=\partial\phi/\partial\eta$ and slowly varying with the axial coordinate ζ so that

$$\frac{\partial\phi}{\partial\zeta}<<\frac{d\theta_b}{d\zeta}\,,\qquad \frac{\partial^2\phi}{\partial\zeta^2}<<\frac{d^2\theta_b}{d\zeta^2} \tag{7}$$

By substituting Eq. (6) into the balance equation Eq. (2) and boundary conditions and making use of the simplifying assumption Eq. (7) one obtains

$$-\frac{Pe\,\alpha}{4}v(\eta)\frac{d\theta_b}{d\zeta}+\frac{\partial^2\phi}{\partial\eta^2}+\frac{\alpha^2}{4}\frac{d^2\theta_b}{d\zeta^2}+18Br\chi^2\rho^2=0 \tag{8}$$

$$\theta_b|_{\zeta=-\beta^-}=0\,,\ \frac{Pe\,\alpha}{4}\frac{d\theta_b}{d\zeta}\bigg|_{\zeta=1+\beta^+}=6Br\chi^2 \tag{9}$$

$$\frac{\partial\phi}{\partial\rho}\bigg|_{\rho=0}=0\,,\ \frac{\partial\phi}{\partial\rho}\bigg|_{\rho=1}=F_w(\zeta) \tag{10}$$

By substituting Eq. (6) into the balance equation Eq. (2), integrating Eq. (6) over the cross section and enforcing only the (second order derivative) simplifying assumption $\frac{\partial^2\phi}{\partial\zeta^2}<<\frac{d^2\theta_b}{d\zeta^2}$ one arrives to the following equation for the dimensionless bulk temperature $\theta_b(\zeta)$

$$-\frac{Pe\,\alpha}{4}\frac{d\theta_b}{d\zeta}+\frac{\alpha^2}{4}\frac{d^2\theta_b}{d\zeta^2}+6Br\chi^2+F_w(\zeta)=0 \tag{11}$$

$$\theta_b(-\beta^-)=0\,,\ \frac{Pe\,\alpha}{4}\frac{d\theta_b}{d\zeta}\bigg|_{\zeta=1+\beta^+}=6Br\chi^2 \tag{12}$$

that can be solved analytically, thus obtaining

$$\begin{aligned}\theta_b(\zeta)&=\frac{4}{Pe^2}\left[g(\zeta)-g(-\beta^-)+\frac{Pe}{\alpha}\left(IF_w(\zeta)+6Br\chi^2(z+\beta^-)\right)\right]\\ g(\zeta,Pe/\alpha)&=\frac{Pe}{\alpha}e^{Pe\zeta/\alpha}\int_{\zeta}^{1}e^{-Pe\zeta'/\alpha}q_w(\zeta')d\zeta'\\ IF_w(\zeta)&=\int_0^{\zeta}q_w(\zeta')d\zeta'\end{aligned} \tag{13}$$

By further substituting the expression for the bulk temperature Eq.(13) into the balance equation Eq. (8) one obtains the following PDE for $\phi(\eta,\zeta)$

$$\frac{\partial^2\phi}{\partial\eta^2}=\left(g(\zeta)+6Br\chi^2\right)\,(v(\eta)-1)+\left(F_w(\zeta)+6Br\chi^2\right)-18Br\chi^2\eta^2 \tag{14}$$

that can be solved analytically for $\phi(\eta,\zeta)$ by enforcing the boundary condition $\partial\phi/\partial\eta|_{\eta=1}=F_w$ and the integral constrain $\frac{1}{2}\int_{-1}^{1}\phi(\eta',\zeta)\,v(\eta')d\eta'=0$ thus obtaining

$$\begin{aligned}\phi(\eta,\zeta)&=\frac{\eta^2}{4}[6Br\chi^2(2+\chi)+g(\zeta,Pe/\alpha)\chi+2F_w(\zeta)]+\\&-\frac{\eta^4}{8}[6Br\chi^2(2+\chi)+g(\zeta,Pe/\alpha)\chi]+C(\zeta)\end{aligned} \tag{15}$$

$$\begin{aligned}C(\zeta)&=-6Br\chi^2\left(\frac{7}{60}+\frac{17}{840}\chi-\frac{2}{105}\chi^2\right)-\\&-g(\zeta,Pe/\alpha)\chi\left(\frac{7}{120}-\frac{2}{105}\chi\right)-F_w(\zeta)\left(\frac{1}{6}-\frac{\chi}{15}\right)\end{aligned} \tag{16}$$

The wall temperature $\theta_w(\zeta)$, accounting for the wall temperature-jump for rarefaction effect, is given by

$$\theta_w(\zeta)=\theta(1,\zeta)+2\,b\,Kn\,\frac{\partial\theta}{\partial\eta}\bigg|_{\eta=1}=\theta_b(\zeta)+\phi(1,\zeta)+2\,b\,Kn\,F_w(\zeta) \tag{17}$$

where $b=\frac{2-F_T}{F_T}\frac{2\gamma}{\gamma+1}\frac{1}{Pr}$, $F_T=1$ (thermal accommodation coefficient), $\gamma=1.4$ and $Pr=0.7$ are assumed as typical values for air [1; 2; 3].

The local Nusselt number $Nu(\zeta)$ in the heating section ($0\le\zeta\le 1$) attains the form

$$\begin{aligned}Nu(\zeta)&=\frac{h\,2H}{k}=\frac{2q_w}{\theta_w-\theta_b}=\frac{2q_w(\zeta)}{\phi(1,\zeta)+2\,b\,Kn\,q_w(\zeta)}=\\&=\frac{210\,q_w(\zeta)}{7q_w(\zeta)\,(5+\chi+30\,b\,Kn)+[6Br\chi^2(2+\chi)+g(\zeta)\chi]\,(7+2\chi)}\end{aligned} \tag{18}$$

and turns out to be a function only of the ratio Pe/α (and not of Pe and α separately). Moreover, the local Nusselt number is independent of the lengths of the upstream and downstream thermally insulated sections.

The two limiting cases Nu_0 for $Pe/\alpha\to 0$ (no axial convection) and Nu_∞ for $Pe/\alpha\to\infty$ (infinitely long channel, Nusselt based on the fully developed temperature profile θ_∞) can be easily recovered by considering that

$$\lim_{Pe/\alpha\to 0}g(\zeta,Pe/\alpha)=0\,,\qquad \lim_{Pe/\alpha\to\infty}g(\zeta,Pe/\alpha)=q_w(\zeta) \tag{19}$$

COMPARISON WITH NUMERICAL SOLUTION

In order to verify the correctness of the analytical solution proposed and to identify the limits of validity in terms of Pe and α, we numerically solved the transport problem Eqs. (2,4-5) with Finite Elements Method (FEM, Comsol 3.5 a).

The convection-diffusion package in stationary conditions has been used. Lagrangian quadratic elements are chosen. The linear solver adopted is UMFPACK, with relative tolerance 10^{-12}.

The number of finite elements is 3×10^5 with a non-uniform mesh. Maximum element size in all the three subdomains ($\zeta < 0$, $0 \leq \zeta \leq 1$ and $\zeta > 1$) is 1×10^{-2}. Smaller elements have been located close to the boundaries. Specifically, a maximum element size of 2×10^{-4} is chosen at the external boundary ($0 \leq \zeta \leq 1, \eta = 1$) and at the internal cross sections ($\zeta = 0, 1$, $0 \leq \eta \leq 1$) i.e. at the internal boundaries between the insulated and the heated regions.

Figures 2 A-B show the comparison between analytical and numerical results for increasing values of *Pe* in terms of the dimensionless bulk temperature $\theta_b(\zeta)$ and wall temperature $\theta_w(\zeta)$ for constant wall heat flux function $q_w = 1$ for $Br = 0.1$, $Kn = 0$.

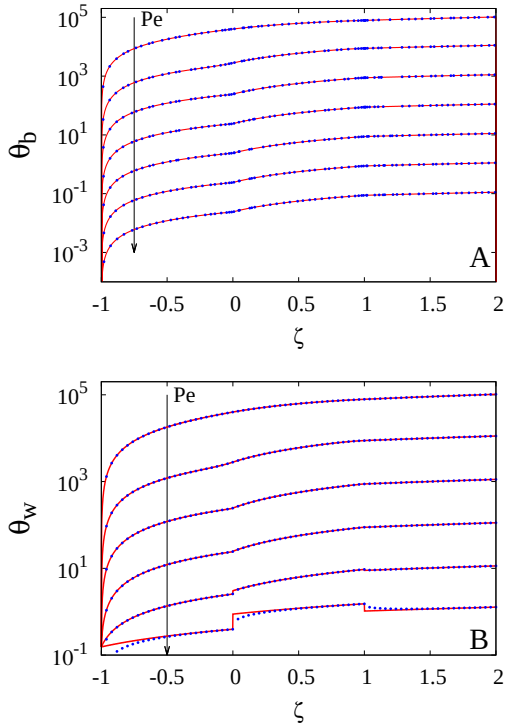

Figure 2. Comparison between numerical (blue dots) and analytical results (red continuous lines) for the constant wall heat flux $q_w(\zeta) = 1$, $Br = 0.1$, $Kn = 0.0$, $\alpha = 0.01$, $\beta^- = \beta^+ = 1$. (A) $\theta_b(\zeta)$ vs ζ, $Pe \in [10^{-2} : 10^5]$. (B) $\theta_w(\zeta)$ vs ζ, $Pe \in [10^{-2} : 10^3]$

It can be observed that the bulk temperature model predictions are actually very accurate in the whole range of Peclet values $Pe \in [10^{-2}, 10^5]$ because, at low *Pe* values the simplifying assumption $\partial^2\phi/\partial\zeta^2 << d^2\theta_b/d\zeta^2$ holds true and, at high *Pe* values, the axial conduction term becomes negligible with respect to the axial convective contribution.

Model predictions for the wall temperature θ_w are accurate for small-intermediate values of *Pe*, $Pe \leq 100$.

The analytical solution for θ_w follows quite closely the numerical solution in the entire range of *Pe* values analyzed, but small errors (related to the simplifying assumption Eq. (7) that fails at discontinuity points $\zeta = 0$ and $\zeta = 1$ for the uniform wall heat flux are amplified when focusing on the spatial behaviour of *Nu* close to $\zeta = 0, 1$ (see Figure 3).

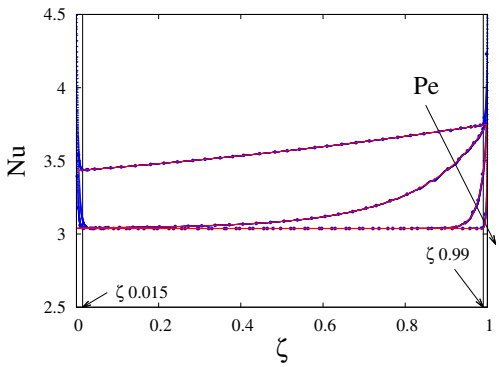

Figure 3. Nu vs ζ. Comparison between numerical (blue dots) and analytical results (red continuous lines) for the constant wall heat flux $q_w(\zeta) = 1$, $Br = 0.1$, $Kn = 0.0$, $\alpha = 0.01$, $\beta^- = \beta^+ = 1$. $Pe \in [10^{-2} : 10^1]$

However, the low accuracy of the analytical solution close to $\zeta = 0, 1$ for a discontinuous wall heat flux has a very small impact of the average Nusselt number $\langle Nu \rangle = \int_0^1 Nu(\zeta')d\zeta'$.

Figures 4 A-B show the excellent agreement between the numerical and the analytical results for $\langle Nu \rangle$ as a function of *Pe* for the exponential wall heat flux function $q_w(\zeta) = n\,e^{-n\zeta}/(1-e^{-n})$ (discontinuous at $\zeta = 0, 1$, decreasing along ζ for $n > 0$ and increasing along the axial coordinate for $n < 0$) for which the integral functions $g(\zeta, Pe/\alpha)$ and $IF_w(\zeta)$ can be analytically evaluated. All data refers to $Br = 0.1$, $Kn = 0$ and an aspect ratio $\alpha = 0.01$ (long-thin channel and long preheating section) and show an excellent agreement with numerical for $Pe \leq 100$.

Limits of validity of the analytical solution

The analytical expression proposed is reliable also for larger values of the aspect ratio (finite-length channel). Figures 5 A-B show the comparison between numerical and analytical results for $\alpha = 0.01, 0.05, 0.1$, in the absence ($Br = 0$) and in the presence ($Br > 0$) of viscous dissipation. It can be observed that different curves corresponding to different aspect ratios saturate towards the same limiting value, corresponding to the average Nusselt number $\langle Nu_\infty \rangle$ evaluated on the basis of the fully developed temperature profile θ_∞. However, the larger is the value of α, the smaller is the range of validity, in terms of *Pe* values, of the fully developed profile and the influence of the thermal developing region must be necessarily accounted for (like in the analytical solution proposed) in order to have an accurate estimate of the average Nusselt number.

Actually, numerical (and analytical) results for $Nu(\zeta)$ as well as for $\langle Nu \rangle$ collapse onto an invariant curve when plotted as function of Pe/α for low-intermediate Peclet values $Pe < 100$, see Figure 5 A, and the asymptotic behaviour sets for $Pe/\alpha \simeq 10^2$.

On the other hand, for high Peclet values, the axial contribution (streamwise conduction) becomes negligible and numerical results for $\langle Nu \rangle$, for different aspect ratios, collapse onto a unique

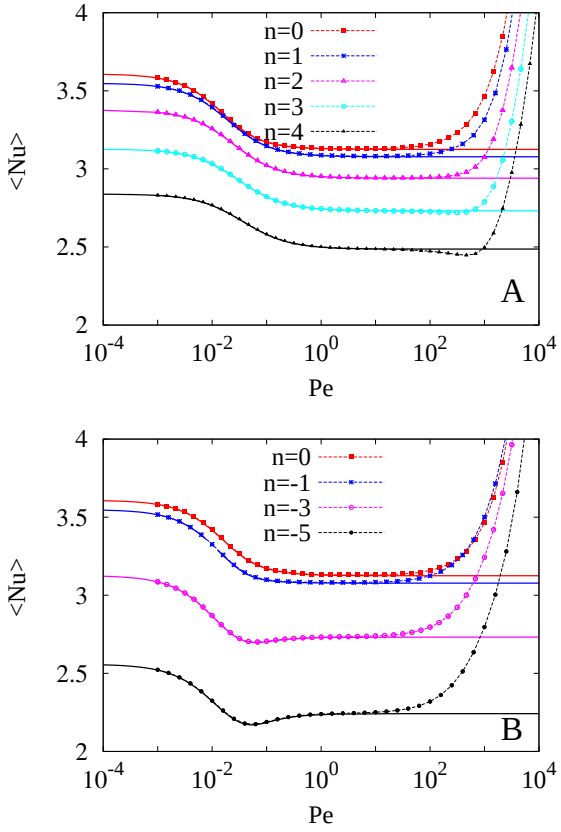

Figure 4. $\langle Nu \rangle$ vs Pe. Comparison between numerical (lines with dots) and analytical results (continuous lines) for the exponential wall heat flux function $q_w(\zeta) = n e^{-n\zeta}/(1-e^{-n})$. $Br = 0.1$, $Kn = 0.0$, $\alpha = 0.01$, $\beta^- = \beta^+ = 1$. (A) $n \geq 0$. (B) $n \leq 0$

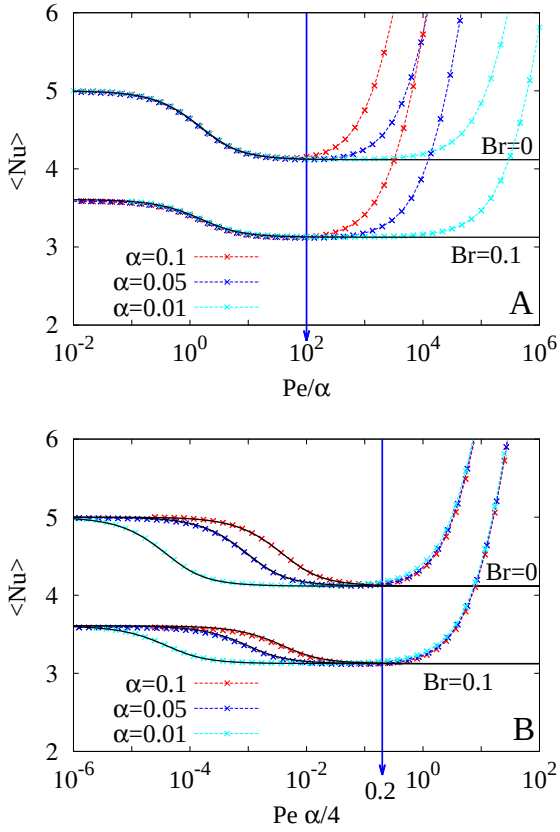

Figure 5. Comparison between numerical (lines with dots) and analytical results (continuous black curves) for the constant wall heat flux function $q_w(\zeta) = 1$ for different values of $\alpha = 0.01, 0.05, 0.1$. $Br = 0, 0.1$, $Kn = 0.0$, $\beta^- = \beta^+ = 1$. (A) $\langle Nu \rangle$ vs Pe/α. (B) $\langle Nu \rangle$ vs $Pe\alpha/4$

invariant curve for $Pe\,\alpha/4 > 0.2$ when plotted as a function of $Pe\,\alpha/4$ (see Figure 5 B).

From these observations it follows that the analytical solution proposed is actually reliable for $0 < Pe \leq 0.8/\alpha$, while the solution $\langle Nu_\infty \rangle$ based on the fully developed temperature profile θ_∞ is valid only in the range $10^2\alpha \leq Pe \leq 0.8/\alpha$, thus reducing to an empty set for $\alpha > 0.089$. Data reported in Figures 5 A-B refer to a case in which $Kn = 0$ but similar considerations can be done in the presence of slip flow and rarefaction effect.

In the next section we analyze the influence of different parameters and of different wall heat flux functions on the average Nusselt number $\langle Nu \rangle$, focusing exclusively on the range of validity of the analytical expression proposed.

INFLUENCE OF WALL HEAT FLUX FUNCTION AND TRANSPORT PARAMETERS

From a preliminary analysis of data reported in Figures 4 A-B we observe that, in presence of dissipation, i.e. $Br > 0$, and for no-slip flow and no rarefaction effects, i.e. $Kn = 0$, the uniform wall heat flux function represent the best heating protocol (larger value of $\langle Nu \rangle$ for low-intermediate values of Pe) with respect to both monotonically increasing or monotonically decreasing (exponential) wall heat flux functions.

For the axially increasing wall heat flux, the average Nusselt number exhibits a minimum for $Pe \simeq 5\alpha$ (see Figure 4 B) and the minimum is more pronounced for increasing values of n, corresponding to an increasing amount of energy furnished close to the channel outlet $\zeta = 1$. For $Br > 0$, no minimum is observed for decreasing wall heat flux functions (see Figure 4 A).

Similar results are obtained, in the presence of viscous dissipation $Br > 0$, for slip flows and rarefaction effects accounted for, i.e. $Kn > 0$. Figure 6 shows the behaviour of $\langle Nu \rangle$ vs Pe/α for $Br = 0.1$ and $Kn = 0.1$, in the Pe range of validity of the analytical solution. Also in this case the uniform wall heat flux function represent the best heating protocol and no minimum is observed for exponentially decreasing wall heat flux functions.

A completely different scenario occurs in the presence of viscous dissipation. Figures 7 shows the behaviour of $\langle Nu \rangle$ as a function of Pe/α for $Br = 0$ and for $Kn = 0, 0.1$. The arrow indicates increasing values of n, in the range $n \in [-5, 5]$. It can be observed that, the larger is n, the larger is the value of $\langle Nu \rangle$ for low-intermediate values of Pe. Therefore, in the absence of dissipation, a decreasing wall heat flux function has to be preferred

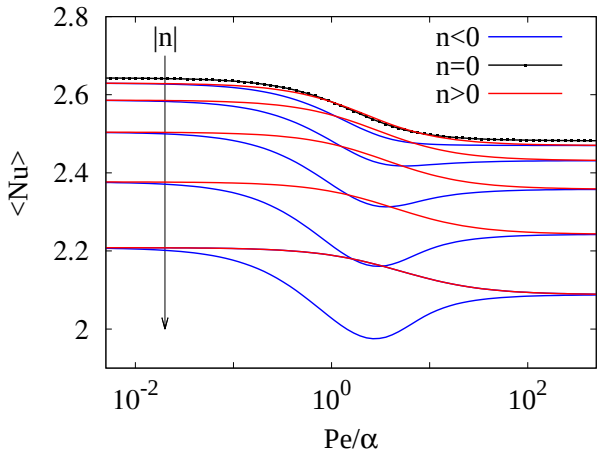

Figure 6. $\langle Nu \rangle$ vs Pe/α for the exponential wall heat flux function $q_w(\zeta) = n e^{-n\zeta}/(1-e^{-n})$. $Br = 0.1$, $Kn = 0.1$, $\beta^- = \beta^+ = 1$. Arrow indicates increasing values of $|n|$, in the range $0 \leq |n| \leq 5$.

to a constant heat flux function and the larger part of energy must be provided at the entrance of the heating section.

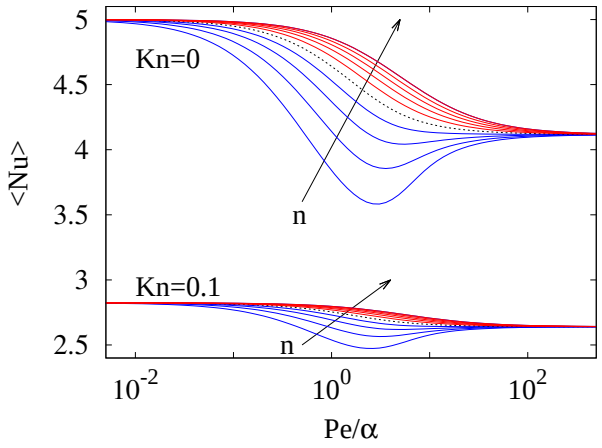

Figure 7. $\langle Nu \rangle$ vs Pe/α for the exponential wall heat flux function $q_w(\zeta) = n e^{-n\zeta}/(1-e^{-n})$. $Br = 0$, $Kn = 0, 0.1$, $\beta^- = \beta^+ = 1$. Arrow indicates increasing values of n in the range $-5 \leq n \leq 5$.

CONCLUSION

In the present paper we propose an analytical solution for the extended Graetz-Nusselt problem in finite-length flat microchannels, including the effects of rarefaction, streamwise conduction and viscous dissipation. The solution takes into account the presence of a thermally insulated upstream section. Different wall heat functions are analyzed.

A classical approach to the problem (see Jeong and Jeong [3; 4] and Tunc and Bayazitoglu [5]) is to solve the non-homogeneous energy balance equation for the dimensionless temperature $\theta(\rho,\zeta)$ by setting $\theta = \theta_1(\rho,\zeta) + \theta_\infty(\rho)$, where θ_∞ is the fully developed temperature profile and θ_1 satisfies an homogeneous partial differential equation that can be solved by the method of separation of variables or by integral transform.

In our case, we focus on finite length channels. Therefore we propose a different "decoupling" of the problem and find more convenient to set the temperature profile θ as the linear combination of the bulk temperature $\theta_b(\zeta)$ and of the auxiliary function $\phi(\rho,\zeta)$, accounting for the dependence of the temperature on the radial coordinate ρ and slowly varying with the axial coordinate ζ. This represents the peculiarity and the strength of our approach to the problem, valid for low-intermediate Peclet values.

The analytical solution is reliable for $Pe < 1/\alpha$, α being the channel aspect ratio.

The solution proposed is valid in the whole range of Brinkman values considered in the microfluidic literature, i.e. $Br \leq 0.1$ and therefore valid also in the absence of dissipation effects. Moreover the solution is valid for slip ($Kn > 0$) as well as for non-slip flows ($Kn = 0$) and therefore also for viscous fluids for which dissipation effects may not be negligible. Actually, a value of Brinkman less than $0.1 - 0.2$ is rather realistic for microfluidic applications and compatible with Peclet numbers less that 100.

Performances of different wall-heat flux functions are analyzed in terms of the averaged Nusselt number $< Nu >$.

In the absence of viscous dissipation, the best heating protocol is a decreasing wall heat flux function, where the larger part of energy is furnished at the entrance of the downstream-heated section.

In the presence of dissipation, i.e. $Br > 0$, the best heating protocol is a uniform wall heat flux and decreasing wall heat flux functions have to be preferred to increasing wall heat flux functions.

REFERENCES

[1] Cetin, B., Yazicioglu, A., and Kakac, S., Slip flow heat transfer in microtubes with axial conduction and viscous dissipation - An extended Graetz problem, *Int. J. Thermal Science*, Vol. 48, 2009, pp 1673-1678.

[2] Cetin, B., and Bayer, O., Evaluation of Nusselt Number for a Flow in a Microtube Using Second-Order Slip model, *Thermal Science*, Vol. 15, 2011, pp. S103-S109.

[3] Jeong, H.-E. and Jeong, J.-T, Extended Graetz problem including streamwise conduction and viscous dissipation in microchannel, *Int. J. Heat and Mass Transfer*, Vol 49, 2006, pp 2151-2157.

[4] Jeong, H.-E. and Jeong, J.-T, Extended Graetz problem including streamwise conduction and viscous dissipation in microtube, *J. Mechanical Science and Technology (KSME Int.J.)*, Vol. 20, 2006, pp 158-166.

[5] Tunc, G. and Bayazitoglu, Y., Heat Transfer in Microtubes with Viscous Dissipation, *Int. J. Heat Mass Transfer*, Vol 44, 2001, pp 2395-2403.

[6] Hennecke, D.H., Heat Transfer by Hagen-Poiseuille Flow in the Thermal Development Region with Axial Conduction, *Wrme - und Stoffbertragung*, Vol. 1, No. 3, 1968, pp. 177-184.

[7] Karniadakis, G.E., Beskok, A., Aluru, N., Microflows and Nanoflows : Fundamentals and Simulation, Springer-Verlag, New York, 2005.